# Hydrolytic stability in hemilabile metal-organic frameworks

*Lauren N. McHugh,[1] Matthew J. McPherson,[1] Laura J. McCormick,[1,2] Samuel A. Morris,[1] Simon J. Teat,[2] Paul S. Wheatley,[1] David McKay,[1] Daniel M. Dawson,[1] Charlotte E. F. Sansome,[1] Sharon E. Ashbrook,[1] Corinne A. Stone,[3] Martin W. Smith[3] and Russell E. Morris[1,4]*

*[1]EaStCHEM School of Chemistry, University of St Andrews, Purdie Building, St Andrews KY16 9ST, UK*

*[2]Advanced Light Source, Lawrence Berkeley National Laboratory, Berkeley, California, 94720, USA*

*[3]Defence Science and Technology Laboratory (Dstl), Porton Down, Salisbury, Wiltshire SP4 0JQ, UK*

*[4]Department of Physical and Macromolecular Chemistry, Faculty of Sciences, Charles University in Prague, Hlavova 8, 128 43 Prague 2, Czech Republic*

# Table of Contents

## 1. Synthetic Procedures for the synthesis of linker precursors and STAM-17-OEt linker:

### 1.1: Dimethyl 5-hydroxy isophthalate:

Synthesised by literature method [1]. A suspension of 5-hydroxy isophthalic acid (53.40 g, 293.20 mmol) in methanol (625 mL) was prepared, to which concentrated sulfuric acid (19.5 mL) was added and the mixture was heated to reflux for 8 hours. The solution was cooled, before being neutralised with saturated aqueous sodium bicarbonate (625 mL) and the solvent was removed under reduced pressure. The residue was suspended in distilled water (100 mL) and was extracted with dichloromethane (approximately 4 L). The organic layers were combined and dried over anhydrous magnesium sulfate, before the solvent was removed under reduced pressure to provide the product as a white solid (48.72 g, 231.80 mmol, 79% yield). $^{1}$H (400 MHz, $d_4$-MeOD) $\delta_C$ 8.11 (t, 1H, aromatic, $J$ = 2.9 Hz, 1.4 Hz), 7.63 (d, 2H, aromatic $J$ = 1.5 Hz), 3.93 (s, 6H, -$CH_3$) ppm.

### 1.2: Dimethyl 5-ethoxy isophthalate:

Synthesised by literature method [2]. Dimethyl 5-hydroxy isophthalate (11.44 g, 54.43 mmol) and potassium carbonate (13.69 g, 99.06 mmol) were dissolved in acetone (260 mL), before iodoethane (5.00 mL, 62.50 mmol) was added and the reaction was heated to reflux for 16 hours. Upon cooling, the solvent was removed under reduced pressure and the resulting solid was taken-up in dichloromethane (300 mL) and distilled water (300 mL). The mixture was extracted with dichloromethane (3 x 200 mL), before the organic layers were washed separately with brine (100 mL) and were dried over anhydrous magnesium sulfate. The solvent was removed under reduced pressure to provide the product as a white solid (12.44 g, 52.22 mmol, 96% yield). $^{1}$H (400 MHz, $d_4$-MeOD) $\delta_C$ 8.18 (t, 1H, aromatic, $J$ = 3.2 Hz, 1.5 Hz), 7.71 (d, 2H, aromatic, $J$ = 1.5 Hz), 4.14 (q, 2H, -$CH_2$-, $J$ = 20.8 Hz, 14.0 Hz, 6.8 Hz), 3.94 (s, 6H, -$CH_3$), 3.94 (s, 3H, -$CH_3$), 1.44 (t, 3H, -$CH_3$, $J$ = 14.0 Hz, 6.8 Hz) ppm.

### 1.3: 5-ethoxy isophthalic acid:

Synthesised by literature method [3]. Potassium hydroxide (11.99 g, 213.70 mmol) and dimethyl 5-ethoxy isophthalate (10.05 g, 42.18 mmol) were dissolved in methanol (250 mL). The solution was heated to reflux for 18 hours, before cooling to room temperature. 2M hydrochloric acid (250 mL) was added to the solution and the resulting precipitate was collected by vacuum filtration. The white solid was repeatedly washed with distilled water until the washings reached pH 6-7 and the product was dried in air for several days (8.55 g, 40.68 mmol, 96% yield)). $^{1}$H (400 MHz, $d_4$-MeOD) $\delta_C$ 8.24 (t, 1H, aromatic, $J$ = 2.8 Hz, 1.6 Hz), 7.74 (d, 2H, aromatic, $J$ = 1.2 Hz), 4.15 (q, 2H, -$CH_2$-, $J$ = 20.8 Hz, 14.0 Hz, 6.8 Hz), 1.45 (t, 3H, -$CH_3$, $J$ = 14.0 Hz, 6.8 Hz) ppm.

## 2. Powder Diffraction:

2.1: Powder X-ray diffraction patterns of STAM-17-OEt:

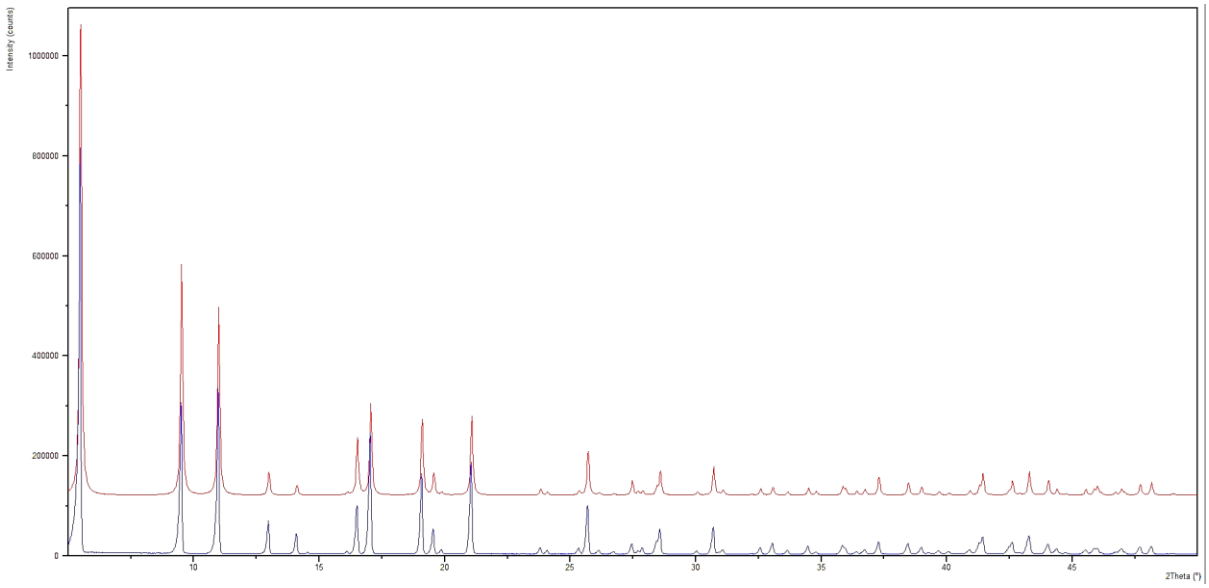

**Fig 2.1.1:** Comparison of experimental (blue line) and simulated (red line) powder X-ray diffraction patterns of STAM-17-OEt. The simulated pattern is obtained from the single crystal data discussed in the manuscript.

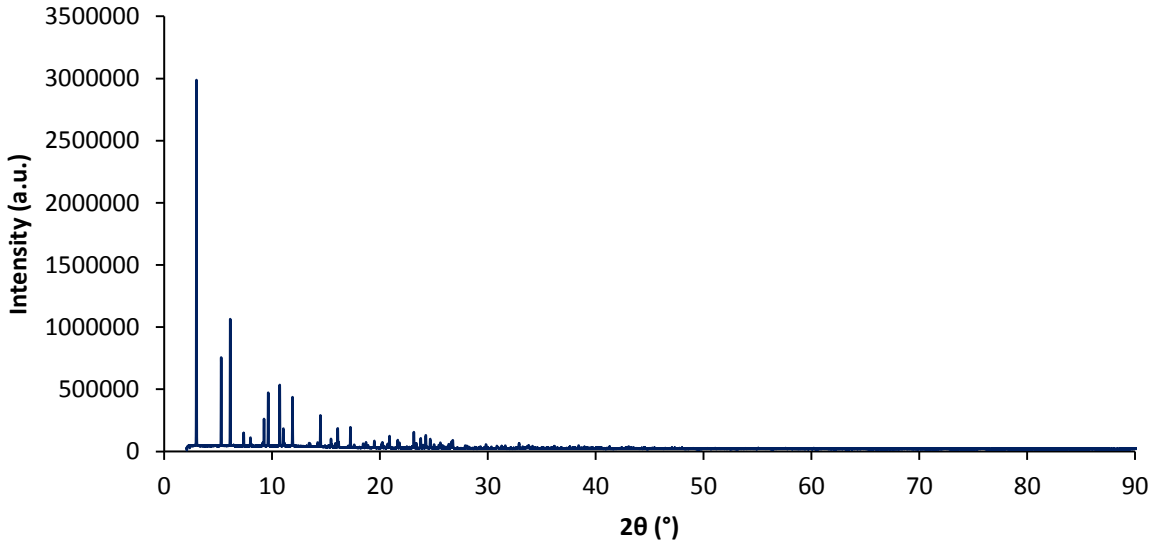


**Fig 2.1.2:** High-resolution synchrotron X-ray (λ = 0.826048 Å) diffraction pattern of as-made STAM-17-OEt.

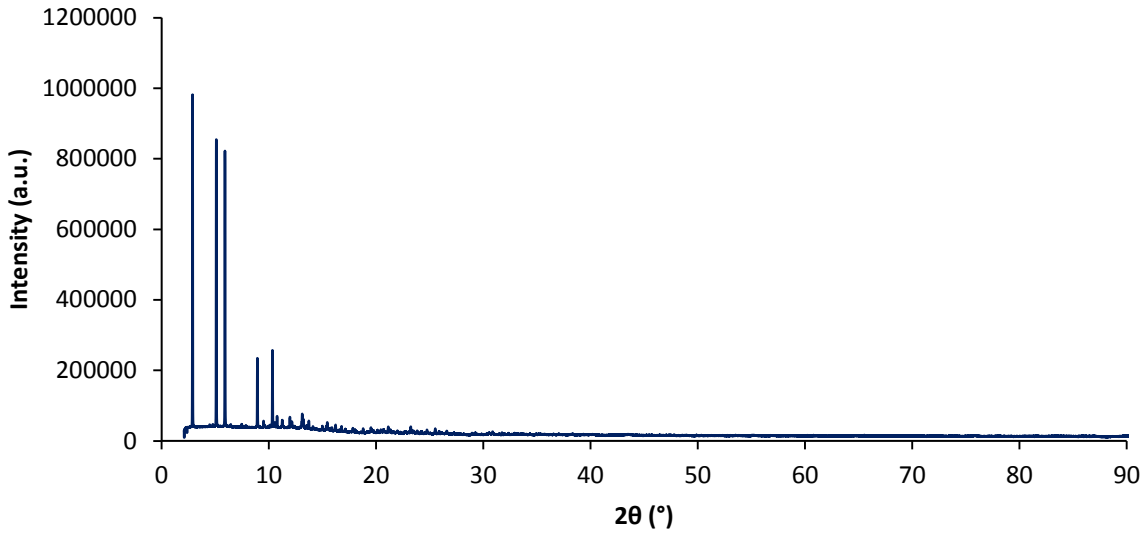


**Fig 2.1.3:** High-resolution synchrotron X-ray (λ = 0.826048 Å) diffraction pattern of dehydrated STAM-17-OEt. The sample was dehydrated under vacuum, at 423 K for 16 hours and sealed in a borosilicate capillary prior to obtaining the measurement.

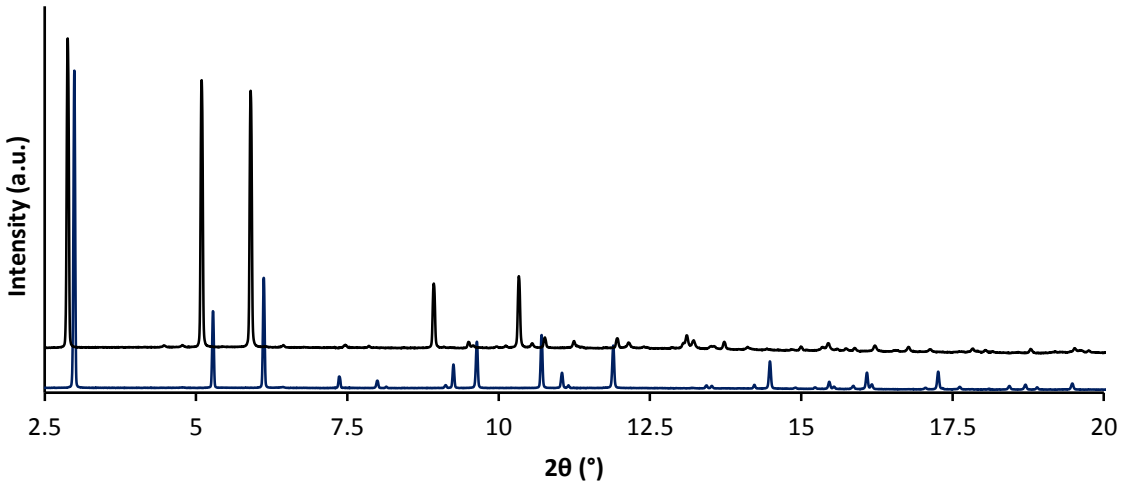


**Fig 2.1.4:** Comparison of high-resolution synchrotron X-ray (λ = 0.826048 Å) diffraction patterns of as-made STAM-17-OEt (blue line) and dehydrated STAM-17-OEt (black line), displayed from 2.5 – 20 2θ, indicating the change in the unit cell upon dehydration of the material.

2.2: Powder X-ray diffraction patterns after water and air exposure:

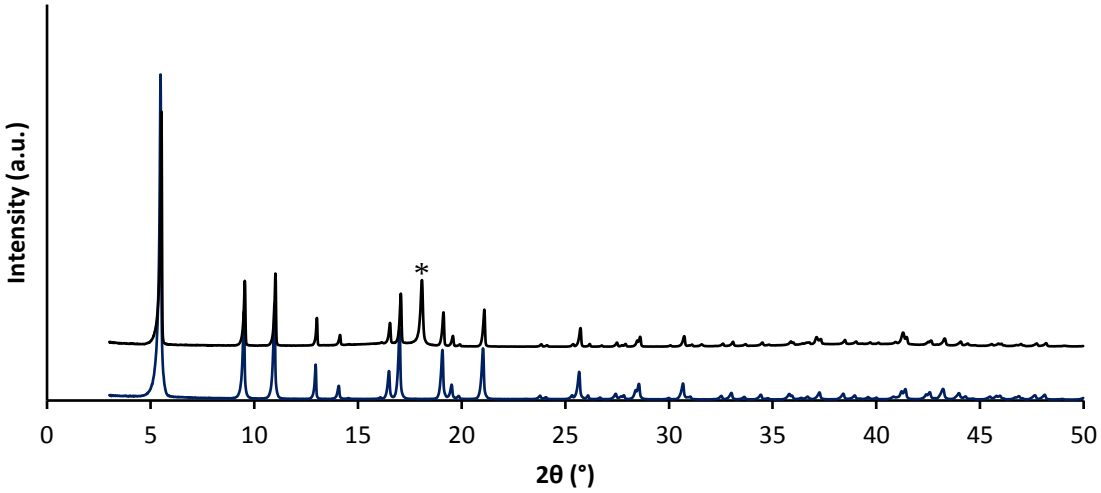


**Fig 2.2.1:** Powder diffraction pattern of as-made STAM-17-OEt (blue line) and STAM-17-OEt after exposure to repeated cycling at 90% RH (black line). The peak marked with a star is a Teflon peak from the insert used during the diffraction experiment. The retention of structure and crystallinity in the sample may be observed. This contrasts with the powder pattern of HKUST-1 in Fig 2.2.2, where the structure has decomposed. See Fig 4.3.1 for more details on the cycling experiment.

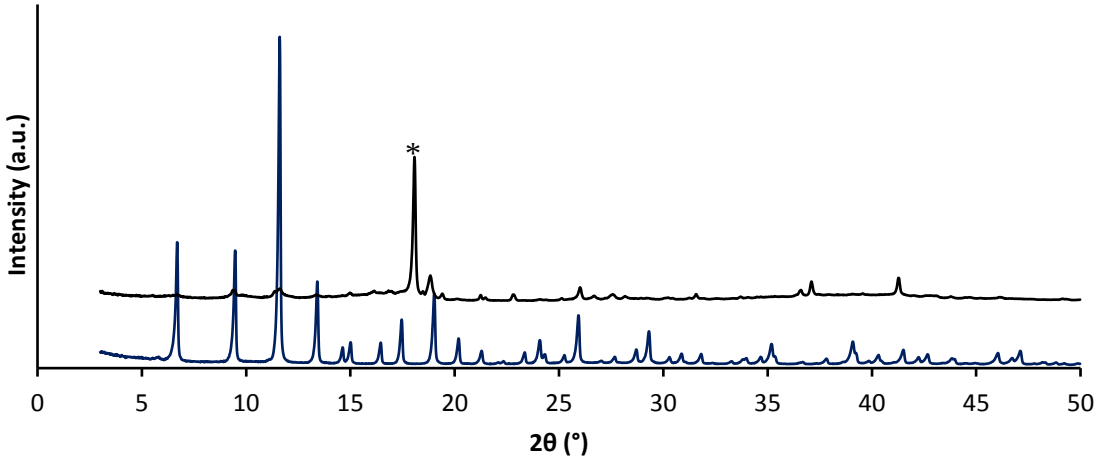


**Fig 2.2.2:** Powder diffraction pattern of as-made HKUST-1 (blue line) and HKUST-1 after exposure to repeated cycling at 90% RH (black line). The peak marked with a star is a Teflon peak from the insert used during the diffraction experiment. The loss of structure and crystallinity in the sample may be observed. See Fig 4.3.2 for more details on the cycling experiment.

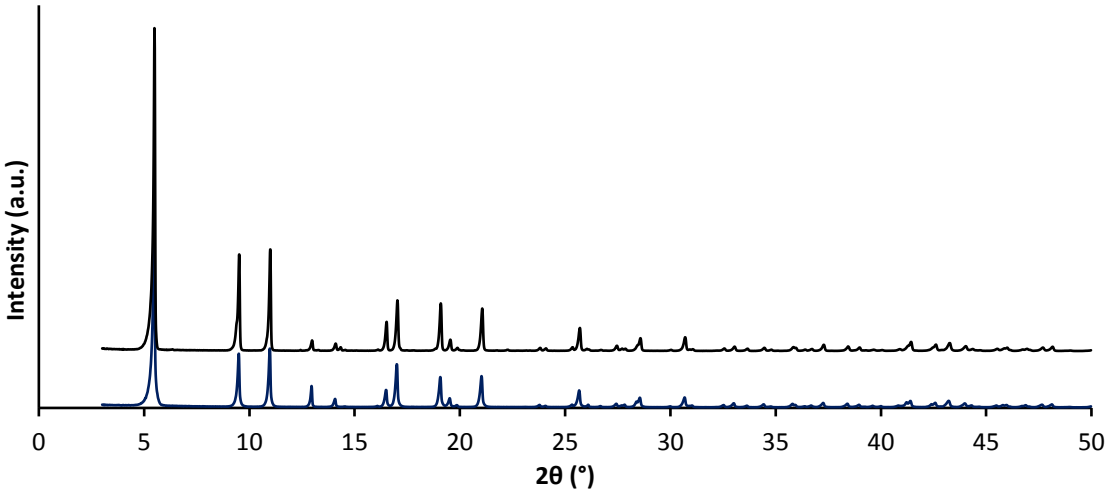


**Fig 2.2.3:** Powder diffraction pattern of as-made STAM-17-OEt (blue line) and STAM-17-OEt after submersion in water for 1 year (black line). The overall retention of structure and crystallinity in the sample may be seen, with very little change observed between the patterns after such prolonged water-exposure.

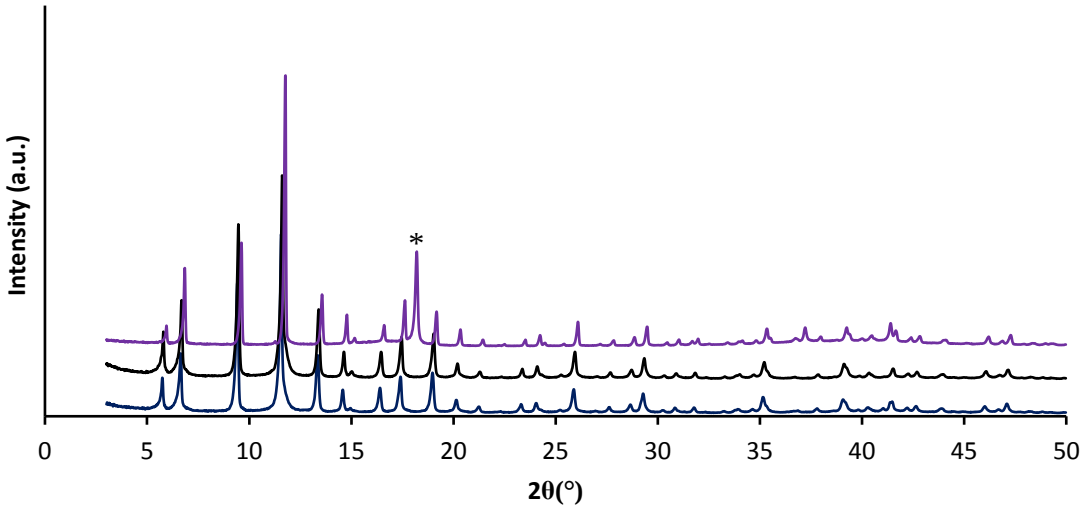


**Fig 2.2.4:** Powder diffraction pattern of as-made HKUST-1 (blue line), as-made HKUST-1 after exposure to air over 2 days (black line) and as-made HKUST-1 after submersion in water for 2 days (purple line). The peak marked with a star is a Teflon peak from the insert used during the diffraction experiment. The structure and crystallinity in as-made HKUST-1 samples after air or moisture exposure is retained, highlighting the greater water-stability of as-made HKUST-1 over dehydrated HKUST-1.

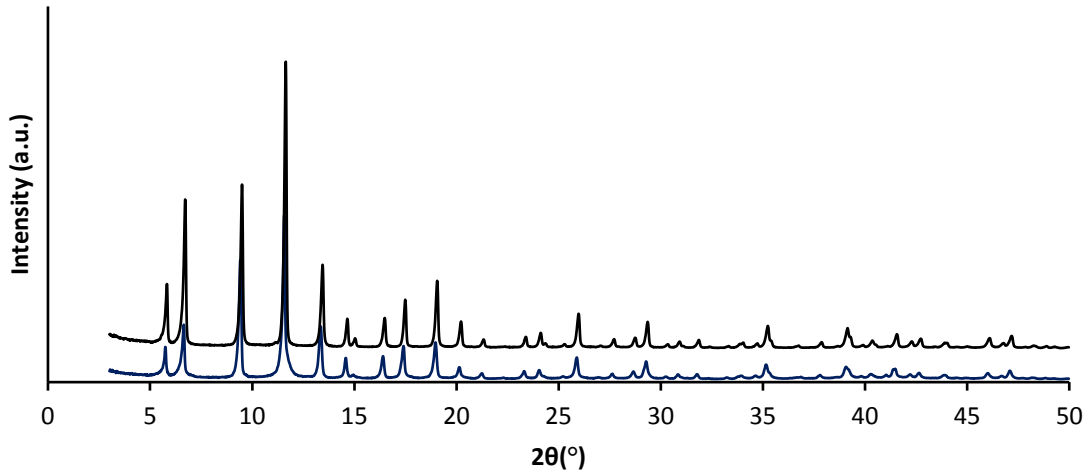


**Fig 2.2.5:** Powder diffraction pattern of as-made HKUST-1 (blue line) and as-made HKUST-1 after exposure to air for over 1 year (black line). No changes are observed between the patterns, further highlighting the stability of as-made HKUST-1.

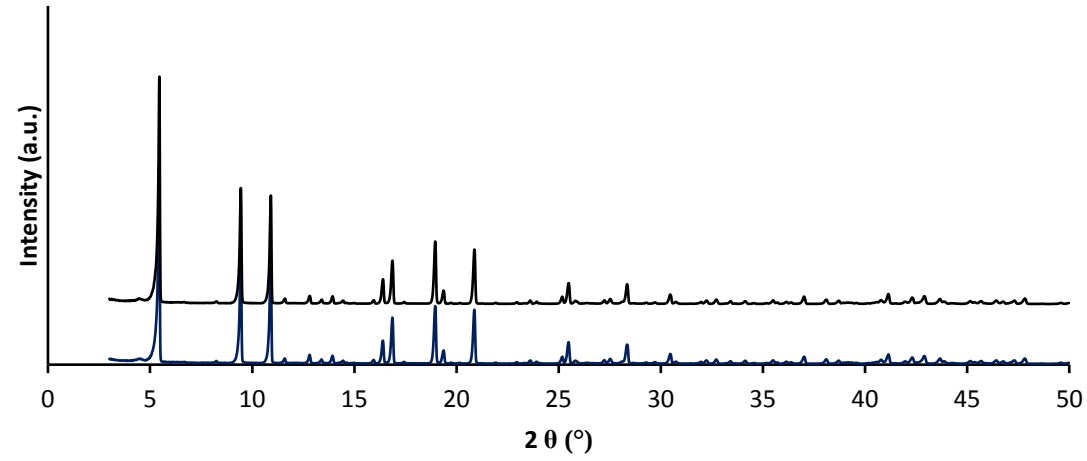


**Fig 2.2.6:** Powder diffraction pattern of as-made STAM-1 (blue line) and activated STAM-1 after submersion in water (black line). No changes are observed between the patterns, highlighting that the hydrolytic stability of the STAM series does not arise due to electronic effects from the ligand's side chain. This hydrolytic stability of STAM-1 may also be observed after water cycling (see Fig 4.3.3 for more details).

## 3. Thermogravimetric Analysis (TGA):

TGA experiments were conducted in air on a Rheotherm TG 1000 M at a fixed rate of 10°C per minute.

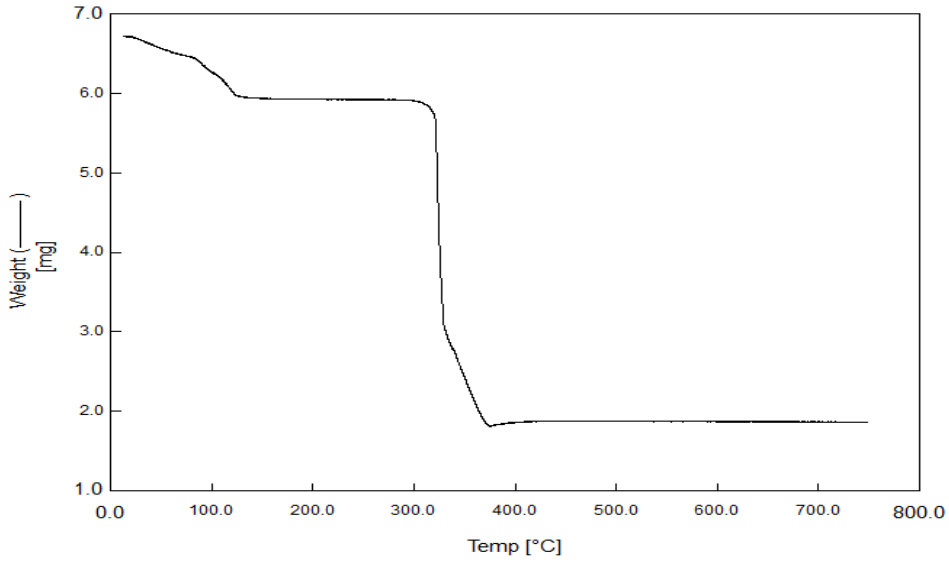


**Fig 3.1:** TGA trace of STAM-17-OEt, showing the loss of water from the structure at approximately 125°C. The dehydrated structure is stable until around 300°C.

## 4. Adsorption Experiments:

### 4.1. BET Analysis:

Nitrogen BET analysis was performed on STAM-17-OEt samples at 77 K on a micromeritics ASAP 2020 Surface Area and Porosity Analyzer and the BET surface areas were calculated using the Rouquerol method.

120 mg samples were activated at either 298 K or 423 K overnight prior to measurement and the values reported show the increase in gas adsorption for the sample activated at elevated temperature:

- BET surface area (activated at 298 K): 4.21 ± 0.06 $m^2/g$
- BET surface area (activated at 423 K): 58.42 ± 0.29 $m^2/g$

## 4.2. Water Adsorption:

Water adsorption at 298 K was monitored using a DVS apparatus, where a sample of material (~20 mg) was placed in a stainless-steel sample pan inside a sealed chamber and the humidity was increased incrementally.

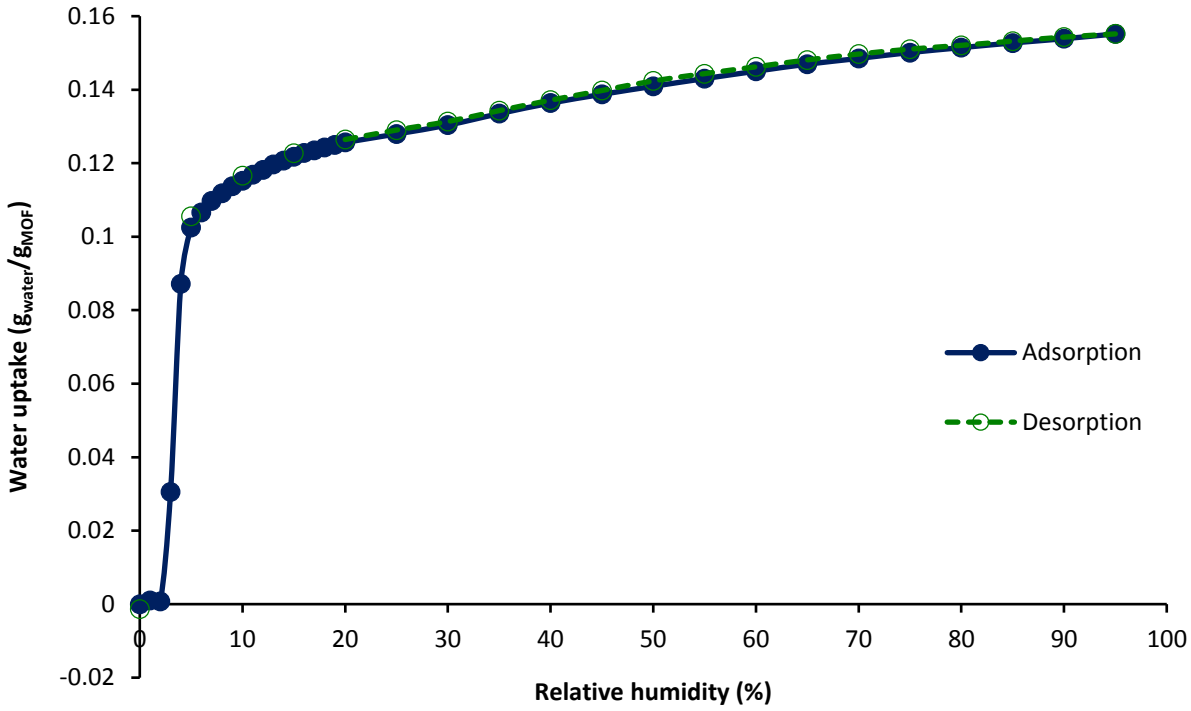


**Fig 4.2.1:** Water adsorption isotherm at 298 K for STAM-17-OEt, showing little to no hysteresis in the desorption branch.

## 4.3. Water Cycling Experiments:

Water cycling experiments were conducted using a DVS apparatus, where samples of material (~20 mg) were placed in a stainless-steel sample pan, inside a sealed chamber and were exposed to multiple vapour adsorption/desorption cycles to 90% relative humidity at 298 K.

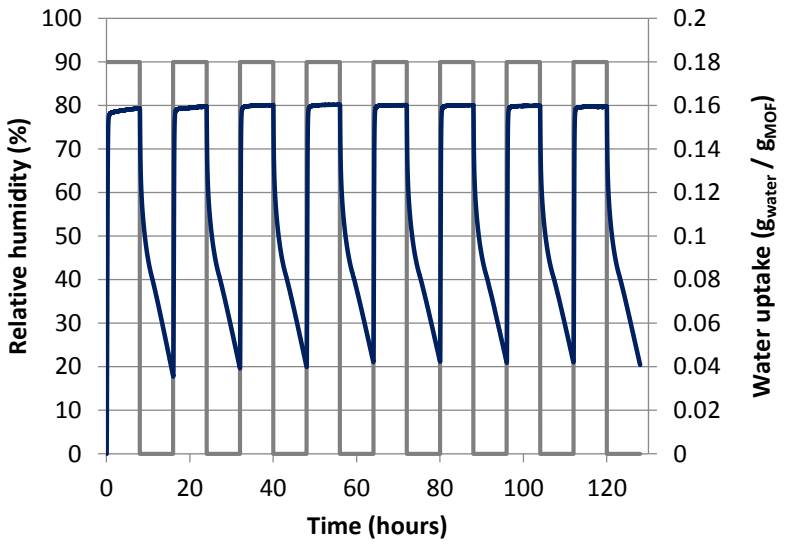


**Fig 4.3.1:** Vapour water stability at 298 K for STAM-17-OEt demonstrated by the change in the sample's water uptake through 8 water adsorption/desorption cycle measurements (blue trace) to 90% relative humidity (grey trace). The chart shows that after the initial water uptake, the sorption capacity in STAM-17-OEt remains constant throughout the experiment. See Fig 2.2.1 for post-cycling powder X-ray diffraction.

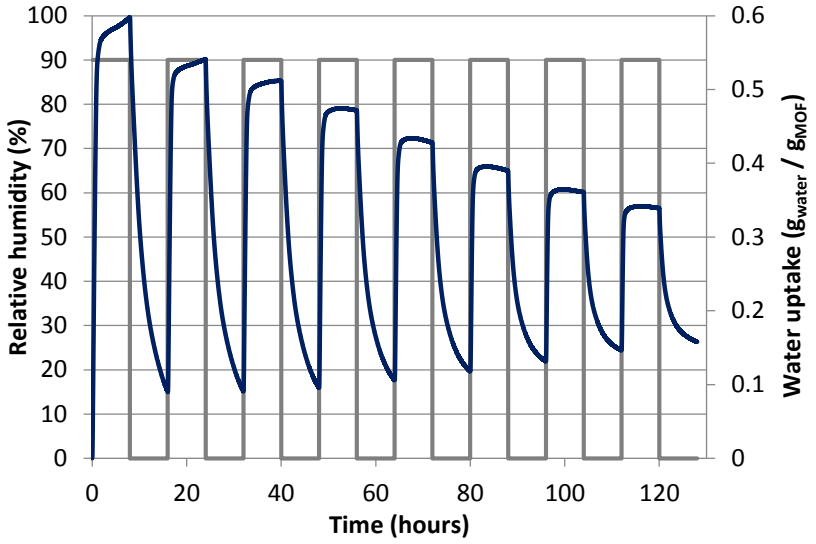


**Fig 4.3.2:** Vapour water stability at 298 K for HKUST-1 demonstrated by the change in the sample's water uptake through 8 water adsorption/desorption cycle measurements (blue trace) to 90% relative humidity (grey trace). The chart shows that after the initial water uptake, the sorption capacity in HKUST-1 decreases throughout the experiment, beginning with the first cycle. See Fig 2.2.2 for post-cycling powder X-ray diffraction.

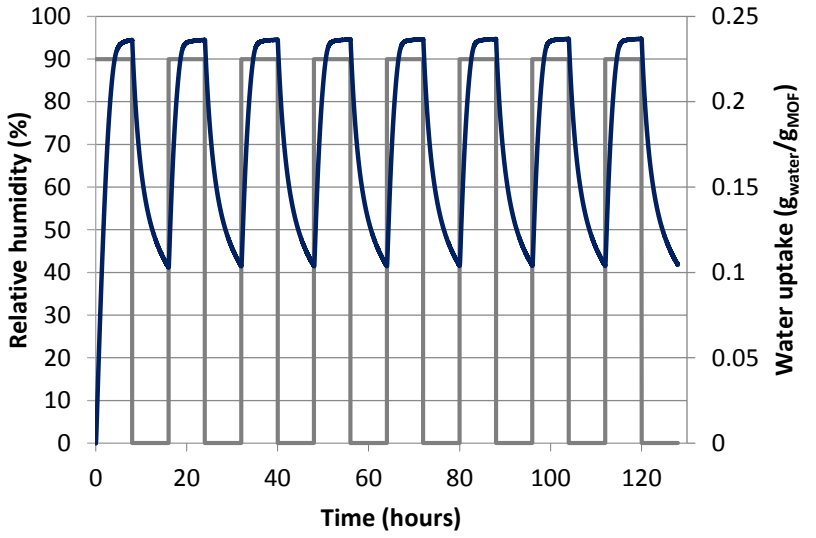


**Fig 4.3.3:** Vapour water stability at 298 K for STAM-1 demonstrated by the change in the sample's water uptake through 8 water adsorption/desorption cycle measurements (blue trace) to 90% relative humidity (grey trace). The chart shows that after the initial water uptake, the sorption capacity in STAM-1 remains constant throughout the experiment, as observed in the isostructural STAM-17-OEt.

## 4.4. Ammonia Micro Breakthrough Experiments:

Experimental conditions for ammonia micro breakthrough experiments are provided in the manuscript.

**Table 4.4.1.**

Summary of ammonia breakthrough times recorded for STAM-17-OEt using 10 mg samples.

| **Conditions:** | **Breakthrough Time (min):** |
|---|---|
| Dry | 27 |
| 80% RH 20 min | 32 |
| 80% RH overnight | 45 |
| 90% RH 5 days | 46 |

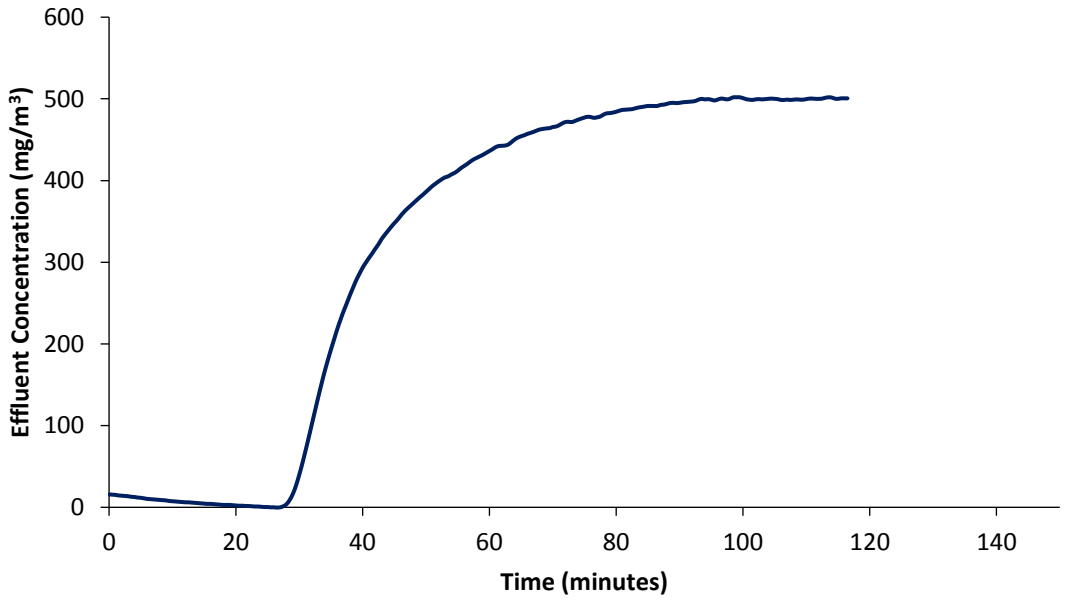


**Fig 4.4.1:** Ammonia breakthrough curve of STAM-17-OEt in a dry ammonia gas stream.

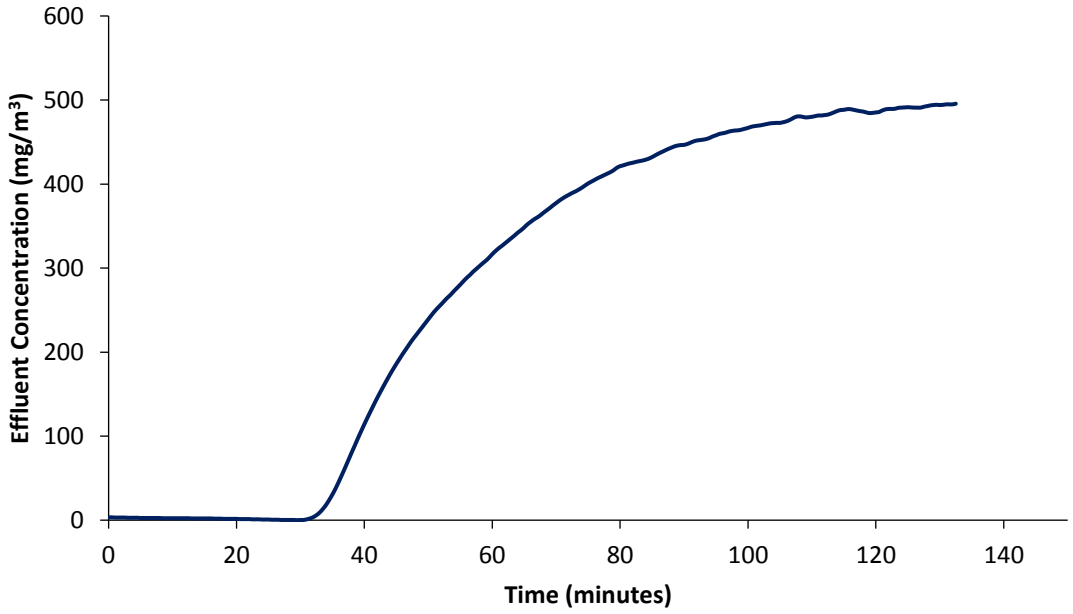


**Fig 4.4.2:** Ammonia breakthrough curve of STAM-17-OEt in an ammonia gas stream at 80% RH after pre-exposure for 20 minutes.

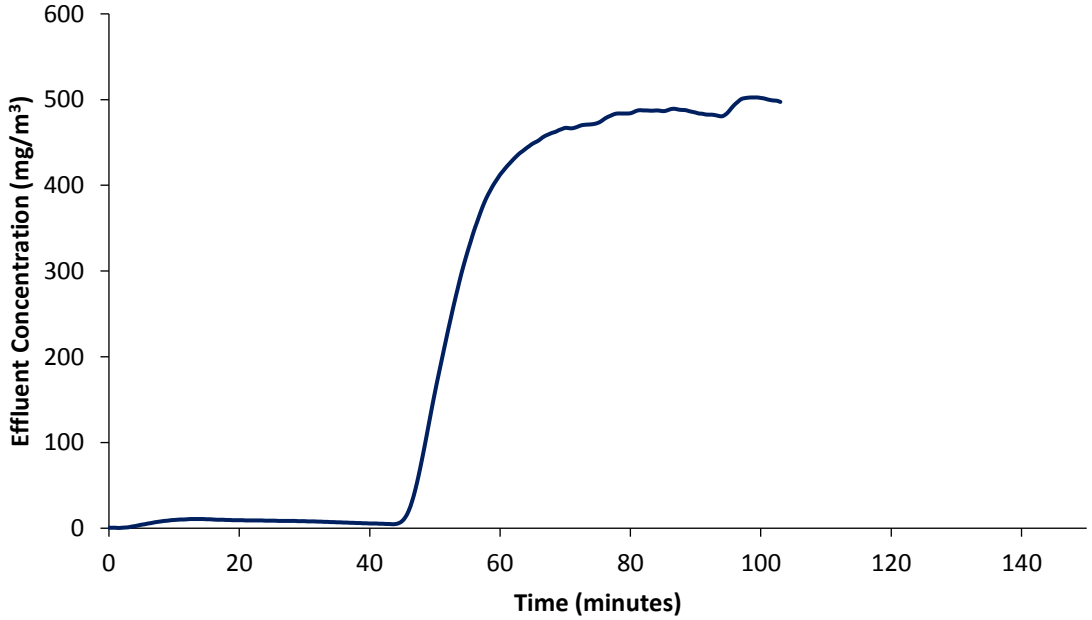


**Fig 4.4.3:** Ammonia breakthrough curve of STAM-17-OEt in an ammonia gas stream at 80% RH after pre-exposure overnight.

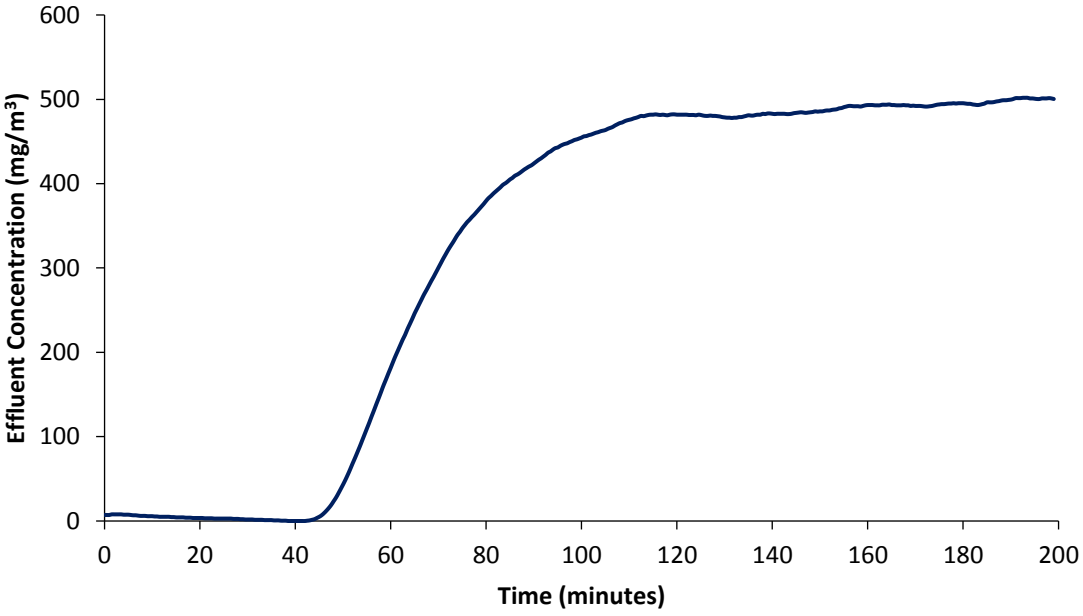


**Fig 4.4.4:** Ammonia breakthrough curve of STAM-17-OEt in an ammonia gas stream at 80% RH after pre-exposure to 90% RH for 5-days.

## 5. Solid-state NMR

Full details of solid-state NMR experiments may be found in the manuscript.

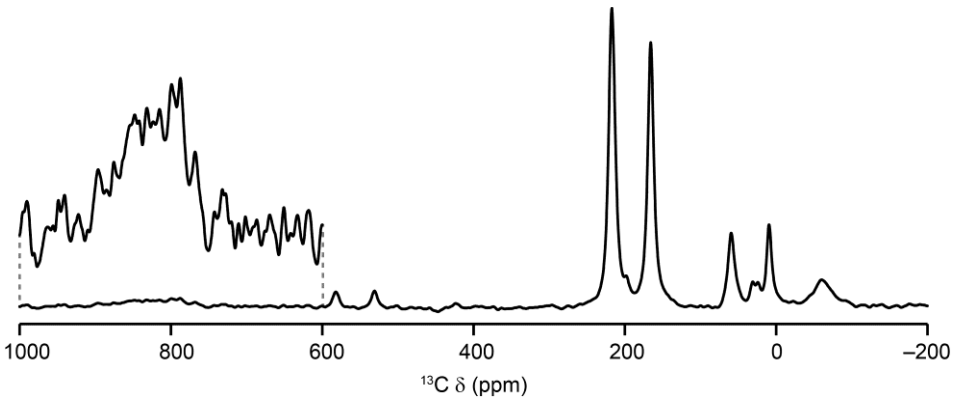


**Fig 5.1:** $^{13}$C (14.1 T, 60 kHz MAS) NMR spectrum of STAM-17-OEt with the inset showing a vertical expansion of the region from 1000 to 600 ppm. The very broad resonance for C1 is observed at ~830 ppm.

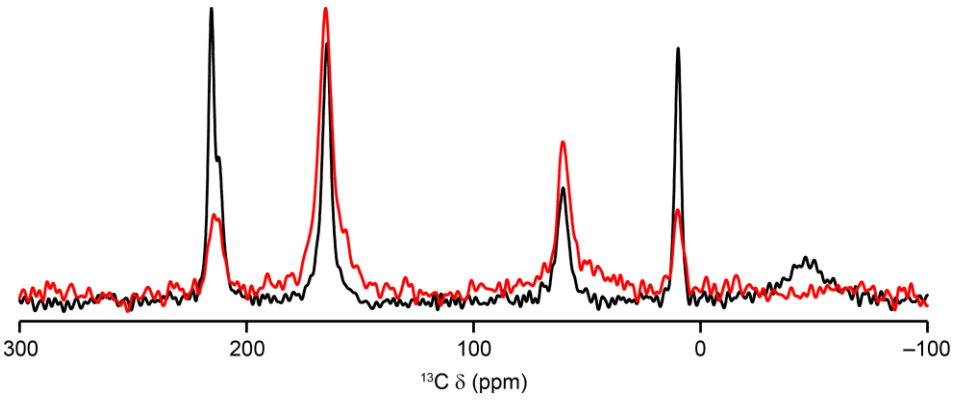


**Fig 5.2:** $^{13}$C (9.4 T, 40 kHz MAS) NMR spectra of STAM-17-OEt recorded with direct excitation (black spectrum) and cross polarisation (CP) with a short spin lock duration of 0.1 ms (red spectrum) to show only $^{13}$C with directly attached $^{1}$H.

## 6. Crystallographic Information

The crystallographic information files for the as synthesized and dehydrated STAM-17-OEt materials are included as .cif files.

### 6.1. As synthesized STAM-17-OEt:

File STAM-17_hydrated_300K.cif contains all the information required for the crystal structure determination of the as-synthesised (hydrated) material.

**Response to CheckCIF A- and B-level alerts in STAM-17_hydrated_300K.cif:**

_vrf_PLAT430_CuEtOipRTair
PROBLEM: Short Inter D…A Contact O4W ..O4W..1.94Å.
RESPONSE: These short contacts are between the oxygen atoms of very low occupancy water molecules. It is unlikely that two of these atoms would occur in such close proximity to each other.

_vrf_PLAT601_CuEtOipRTair
PROBLEM: Structure Contains Solvent Accessible VOIDS of 209 Å$^3$.
RESPONSE: This is correct, there are two series of voids, one of which is hydrophilic and contains disordered water molecules. The second series of channels is hydrophobic and is empty of solvent water molecules.

### 6.2. Dehydrated STAM-17-OEt:

File STAM_17_dehydrated_vac_300K.cif contains all the information required for the crystal structure determination of the dehydrated material.

**Response to CheckCIF A- and B-level alerts in STAM_17_dehydrated_vac_300K.cif:**

_vrf_THETM01_CuEtOipRTvac
PROBLEM: The value of sine (theta_max) / wavelength is less than 0.550.
RESPONSE: Upon dehydration, the crystal undergoes a single-crystal-to-single-crystal transformation. The new structure contains large voids and does not diffract out beyond a resolution of 0.95 Å. The data was truncated to this resolution at the integration stage of the data processing.

_vrf_DIFMN02_CuEtOipRTvac
PROBLEM: The minimum difference density is < -0.1*ZMAX*1.00.
RESPONSE: This is correct. A visual inspection of the residual electron density suggests that the Cu3-Cu4 copper acetate lantern and the C16-C21 5-ethoxy isophthalate ligand are disordered over two sites due to incomplete conversion of the crystal from the hydrated to the dehydrated phase. Attempts were made to model this disorder, however, they gave an occupancy ratio of 93:7, so these attempts were abandoned as modelling structural disorder with such a minor occupancy created new problems with the refinement and, with less than 10% occupancy, any additional chemical information is unlikely to be reliable.

_vrf_PLAT201_CuEtOipRTvac
PROBLEM: Isotropic non-H Atoms in Main Residue(s) .....48 Report.
RESPONSE: This is correct, only two atoms (Cu1 and Cu2) have been refined anisotropically. Attempts were made to refine all four copper atoms and the oxygen atoms bound to them with anisotropic thermal displacement parameters, however these almost exclusively became non-positive definite. Making further atoms anisotropic would have resulted in a data to parameter ratio of less than 10. Given the strain that the crystal has been subjected to, and the probable disorder described above, it is reasonable to assume that the tendency of these atoms to go NPD is due to an incomplete conversion of the crystal to the dehydrated phase. While it was possible to use SIMU, RIGU and DELU commands to prevent these atoms from going NPD, doing so on such a large scale would effectively render the anisotropic refinement meaningless. As such, it was decided to leave the oxygen atoms, Cu3 and Cu4 with isotropic thermal displacement parameters.

_vrf_PLAT410_CuEtOipRTvac
PROBLEM: Short Intra H...H Contact H4..H6B. 1.79 Å.
RESPONSE: These hydrogen atoms have been included at their geometrically estimated positions. The orientations of the methylene groups relative to the aromatic core of the ligand bring the hydrogen atoms close together. Given the poor data quality, it is likely that the terminal methyl groups, and as an extension the methylene hydrogen atoms, are rotationally disordered. While it is possible to place restraints on the data to force the hydrogen atoms apart, I have decided not to do this as there are already a comparatively large number of bond length and SIMU/DELU/RIGU restraints on the data and I did not want to impose constraints onto the orientation of the ethyl group relative to the aromatic core unnecessarily.

_vrf_PLAT972_CuEtOipRTvac
PROBLEM: Check Calcd Residual Density 0.76Å From Cu3 -4.3 eÅ$^{-3}$.
RESPONSE: The placement of the largest two peaks of electron density, and these largest negative peaks of electron density surrounding the Cu3-Cu4 copper acetate lantern strongly suggest that this group, and the C26-C31 5-ethoxy isophthalate ligand are disordered due to incomplete conversion between the hydrated and dehydrated crystal phases. Attempts to model this disorder did account for these positive and negative peaks of electron density but gave an occupancy ratio of 93:7. The 7% occupancy of the minor residual occupancy is too low to obtain any meaningful structural information, so further modelling of this minor orientation

was abandoned.

_vrf_PLAT098_CuEtOipRTvac
PROBLEM: Large Reported Min. (Negative) Residual Density -4.10 eÅ$^{-3}$.
RESPONSE: The placement of the largest two peaks of electron density, and these largest negative peaks of electron density surrounding the Cu3-Cu4 copper acetate lantern strongly suggest that this group, and the C26-C31 5-ethoxy isophthalate ligand are disordered due to incomplete conversion between the hydrated and dehydrated crystal phases. Attempts to model this disorder did account for these positive and negative peaks of electron density but gave an occupancy ratio of 93:7. The 7% occupancy of the minor residual occupancy is too low to obtain any meaningful structural information, so further modelling of this minor orientation was abandoned.

_vrf_PLAT220_CuEtOipRTvac
PROBLEM: Non-Solvent Resd 1 C Ueq (max) / Ueq (min) Range 10.0 Ratio.
RESPONSE: This is correct. Of the four unique EtOip2- ligands, two are bound only to the Cu1-Cu2 copper acetate lantern (and have low thermal displacement parameters) whilst two connect copper acetate lanterns of different types. The slight disorder of the Cu3-Cu4 copper acetate lantern has been described elsewhere in this cif, and there is evidence that this disorder also affects the EtOip2- ligands bound to the lantern unit. The data quality is less than ideal and further modelling of this disorder was not pursued.

_vrf_PLAT341_CuEtOipRTvac
PROBLEM: Low Bond Precision on C-C Bonds .....0.06692 Å.
RESPONSE: The resolution of the diffraction data is less than optimal, due to the large (now empty) channels in the crystal and the stress to which the crystal has been subjected. This, coupled with the chance of incomplete conversion of the crystal from the hydrated to dehydrated phase, leads to a lower than ideal bond precision. Despite these issues, the connectivity of the coordination framework is unambiguous.

_vrf_PLAT601_CuEtOipRTvac
PROBLEM: Structure Contains Solvent Accessible VOIDS of 113 Å$^3$.
RESPONSE: This is correct, the crystal has been dehydrated under dynamic vacuum and all coordinated water molecules have been removed from the copper acetate lanterns. A SQUEEZE analysis on the data for residual electron density analysis only (no refinement has been performed against the SQUEEZED data) showed 77 residual electrons per unit cell, which corresponds to 4 electrons remaining per Cu centre, or 0.43 water molecules per Cu(EtOip) formula unit.

6.3. Scanning Electron Microscopy Images:

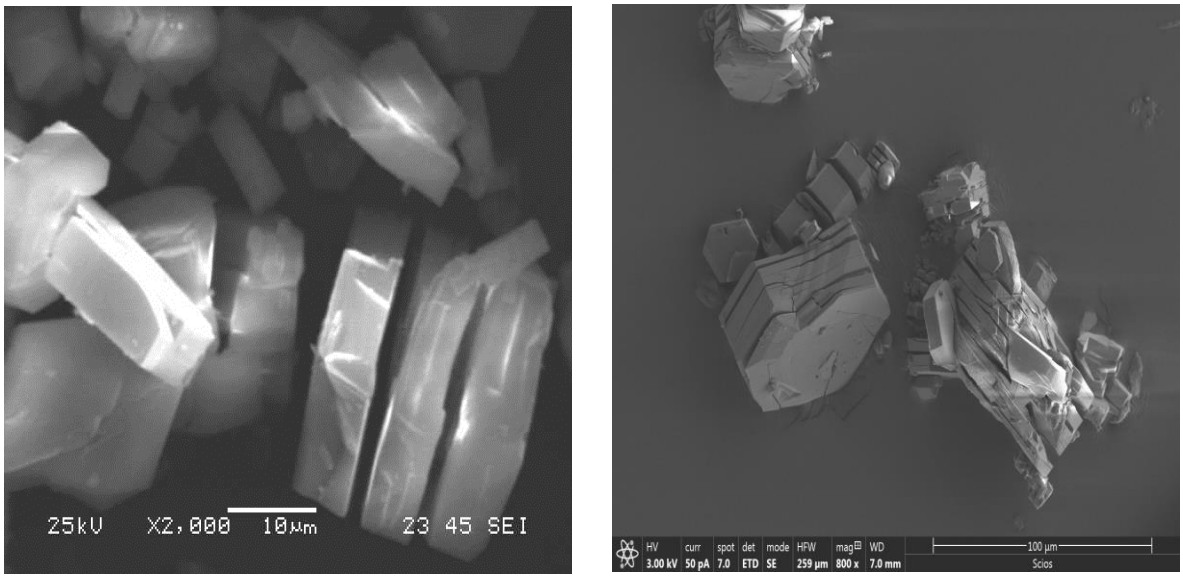


**Fig 6.1:** Scanning Electron Microscopy (SEM) images of STAM-17-OEt crystals.

## References:


1. Chucholowski, A., *et al*. Sulfuric acid esters of sugar alcohols. U.S. Patent US5521160A (1996).

2. Abourahma, H., *et al*. Crystal Growth & Design **3**, 513-519 (2003).

3. Gibson, H.W., *et al*. Rotaxanes from Tetraclams. Macromolecules **45**, 1270-1280 (2012).